

The MROI fringe tracking system: Camera hardware modifications to integrate the SAPHIRA detector

R. Ligon^{*a}, C. Salcido^a, D. Buscher^b, M.J. Creech-Eakman^a, C. Haniff^b, F. Santoro^a, C. Jurgenson^c, T.M. McCracken^d, L. Schmidt^e, J.S. Young^b

^aMagdalena Ridge Observatory, New Mexico Institute of Mining and Technology, 801 Leroy Place, Socorro, NM, USA 87801; ^bCavendish Laboratory, University of Cambridge, JJ Thomson Avenue, Cambridge, UK, CB30HE; ^cGenesis Engineering Solutions, Inc., 4501 Boston Way, Lanham, MD, USA 20706; ^dBall Aerospace, 1600 Commerce Street, Boulder, CO, 80103; ^eDept. of Physics and Astronomy, Texas A&M University, 4242 TAMU, College Station, TX, USA 77843

ABSTRACT

The ICoNN (Infrared Coherencing Nearest Neighbors) fringe tracker system is the heart of the Magdalena Ridge Observatory Interferometer (MROI). It operates in the near-infrared at H or K_s in such a way that the light being used by the fringe tracker can phase up the interferometric array, but not steal photons from the scientific instruments of the interferometer system. It is capable of performing either in group delay tracking or fringe phase tracking modes, depending on the needs of the scientific observations.

The spectrograph for the MROI beam combiner was originally designed for the Teledyne PICNIC array. Developments in detector technology have allowed for an alternative to the original choice of infrared array to finally become available – in particular, the SAPHIRA detector made by Selex. Very low read noise and very fast readout rates are significant reasons for adopting these new detectors, traits which also allow relaxation of some of the opto-mechanical requirements that were needed for the PICNIC chip to achieve marginal sensitivity. This paper will discuss the opto-mechanical advantages and challenges of using the SAPHIRA detector with the pre-existing hardware. In addition to a design for supporting the new detector, alignment of optical components and initial testing as a system are reported herein.

Keywords: MRO, interferometry, spectrograph, fringe tracker, camera

1. INTRODUCTION

At the backend of the MROI, is a fringe tracking system, ICoNN, that utilizes a very low dispersion spectrograph for tracking fringes between pairs of sequential telescopes. Previous papers showed the design of the ICoNN system as a whole and specific design attributes of the spectrograph.^{1,2} Other papers have discussed experiments that show the functionality and performance of the beam combining subsystem.^{3,4} Now the focus is on building and testing the spectrograph which is designed to operate in both H band and K_s band. This paper will concentrate on H-Band which is the primary band for our requirements with the Air Force Research Laboratory (AFRL).

Our partners at Cambridge are obtaining a SAPHIRA detector for use in the MROI spectrograph. This paper will point out the differences of the SAPHIRA detector that will require changes, some of which are advantageous, to the optical alignment and optical performance of the camera. We will then discuss the progress in alignment and testing of the spectrograph in anticipation of the SAPHIRA detector arriving in early 2019.

2. DETECTOR DIFFERENCES

The SAPHIRA detector has many differences with older technologies which makes it a better choice of detector for many instruments. The biggest advantage to the MROI is the very low read noise.^{5,6} Not only will it allow us to have better sensitivity, but the tolerances on alignment become much more relaxed.

The PICNIC detector, with much higher read noise (canonically 10's of electrons per read), forced the spectra to be aligned on one column of pixels and for the encircled energy to be contained in a width of one pixel.

*rligon@mro.nmt.edu;

The initial design used array focus off-axis parabolas (OAP's) that were actively actuated by piezos so that the beams could be centered on one pixel in the direction orthogonal to the dispersion axis to minimize read noise. This can be relaxed to three pixels co-added with the SAPHIRA detector and thus the piezo actuation is no longer required. Not only does this simplify the inside of the dewar but it will also help with the efficiency of the automated alignment procedure.

Of course nothing comes for free as we had to re-engineer the mechanical design to fit the new form factor of the detector and its electronics board. The array has a smaller form factor than the PICNIC array as shown in figure 3. We will discuss the impact of these two parameters in the following sections.

2.1 Accommodating the different form factor of the electronics board

Installing an upgraded array comes with the knowledge that the upgrade needs to fit within the old envelope. Figure 1 shows the beam paths for the first three of the five possible interferometric combinations handled by each ICoNN spectrograph. All five beams were used for analysis but only three beam combinations are shown that will be used for the first phase of the project with the AFRL. The spatial filter unit is not installed in the image and a Xenics Bobcat is being used for warm testing at the approximate array location. The H-Band direct view prisms (DVP) are installed (the mount for the K_s direct view prisms is facing out of the page).

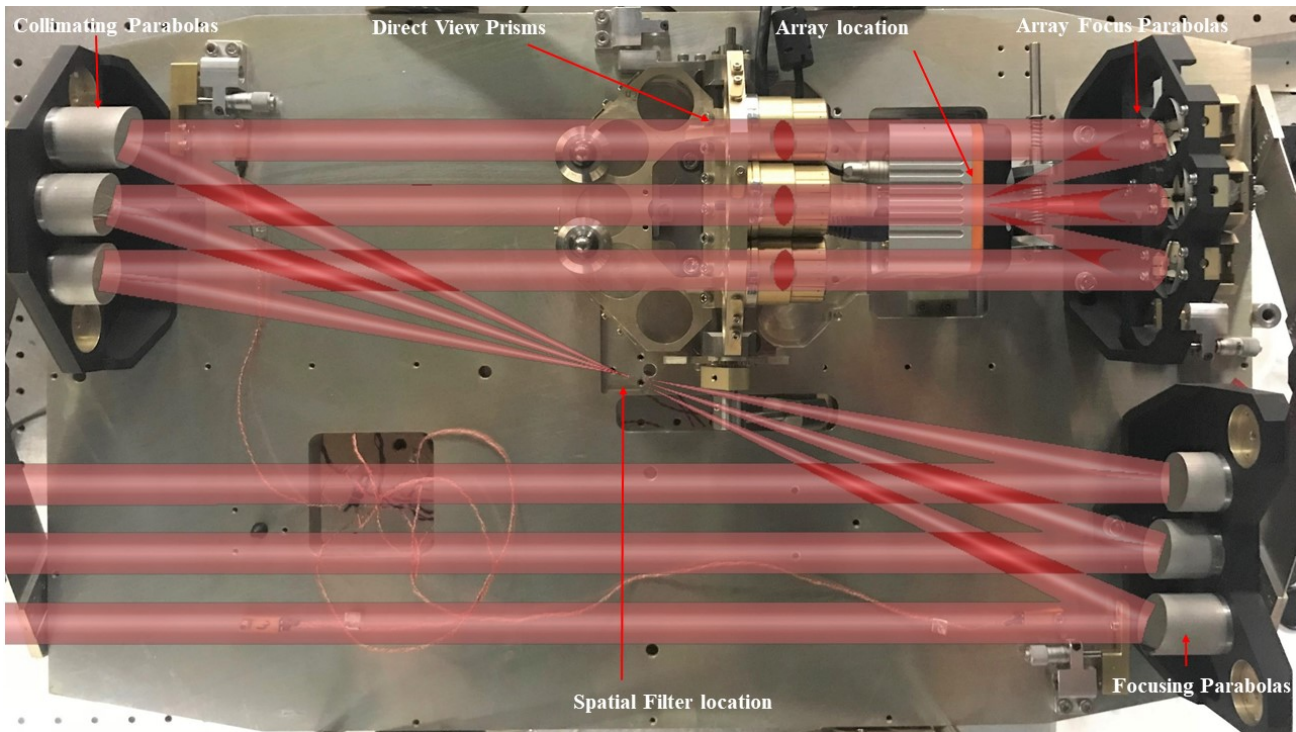


Figure 1. ICoNN spectrograph showing the first three beam paths through the dewar. Beams shown are referred to beam paths 2, 3, and 4. A warm test camera is in the place of the focal plane array in this photograph.

The SAPHIRA electronics board required a new housing and adaptation to the existing mounting hardware to fit. Figure 2 shows the relative differences in size of the electronics housing for the SAPHIRA array (left) versus the PICNIC array (right) in relation to the optical beams paths that travel by the unit as shown in figure 1. The new unit is tilted by 10 degrees from the original design to allow margin between the clear aperture of the beams and the housing as shown in figure 3. Since this angle is in the direction of dispersion, there is a 10% reduction in the amount of dispersion that results from this change in the projected angle onto the array. Also, the array was initially perpendicular to the parent optical axis; this caused the shorter wavelengths to arrive at the array plane before focus and for the longer wavelengths to arrive at the array plane after focus. Since the beams are coming in at a compound angles (except the middle path), the spectra appear to be rotated. The DVP's were rotated to compensate. Tilting the focal plane changed the rotation. The old and new DVP rotations required are shown in Table 1.

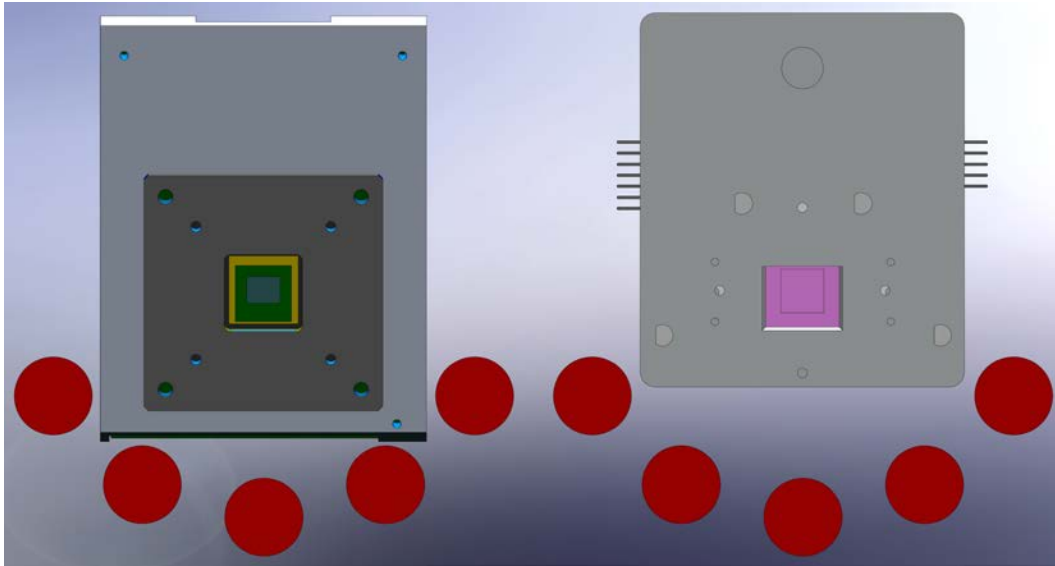


Figure 2. Image showing the SAPHIRA board with housing on the left and the PICNIC board with housing on the right. The red circles represent the clear apertures of the optical beam paths as they pass the detectors going from DVP to focus parabolas.

Table 1: DVP rotation (degrees) given a 10 degree array mount tilt

	OAP 1	OAP 2	OAP 3	OAP 4	OAP 5
Original	-4.8	-5.3	0	5.3	4.8
10 Degrees	.7	-1.7	0	1.7	-0.7

2.2 Accommodating the different form factor of the array

The PICNIC array is 256x256 pixels with a 40 micron pixels or approximately 10.2 mm². The SAPHIRA array is 320x256 pixels with 24 micron pixels or approximately 7.7 mm x 6.1 mm. The original focus OAP's were set to give the spectral separation shown in figure 3. Moving the spectra to fit on the SAPHIRA detector, by tilting the OAP's, requires a tilt of approximately 1.5 degrees and causes a large amount of aberration. A better approach requires moving focus OAP's 1,2,4,5 in by 0.7 mm as shown by the red arrows in figure 3. This modification will be done in the future after testing the first 3 beam paths since the outer beams are not required until the next phase of the project.

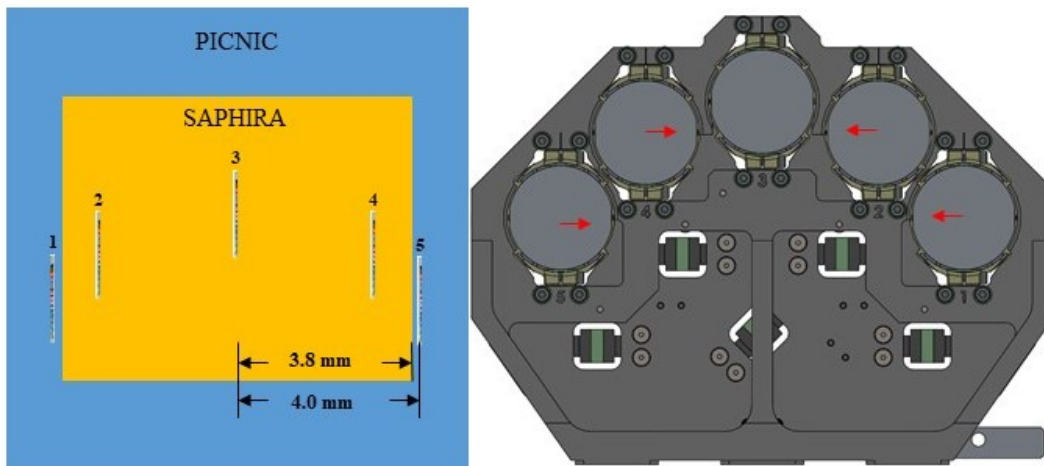


Figure 3. Image showing location of the spectra from all 5 beams overlaid onto a schematic of the footprint of both detectors (left). On the right, image of the focus OAP mount showing direction the outward parabolas to move so that all spectra fit onto the SAPHIRA array.

3. OPTICAL ALIGNMENT AND TESTING

The fringe tracker system has three parts to the alignment scheme. The first part of the scheme aligns the external beams of the combiner to produce fringes. The second part allows the combined beams to be aligned to the spectrograph via a pair of mirrors per beam in a periscope type arrangement. The third part aligns the spectrograph itself. This paper focuses on the third part assuming the first two parts are done and are satisfactory to align the beams to the spectrograph.

The initial design of the instrument led to tight tolerances. The spatial filter parabolas are designed to have only one degree of freedom, rotation of the common mount around a locating pin in the cold plate (Figure 1). Off-axis distance, rotation, focus, and tip are fixed and common to all five paths. The array focus parabolas have that same mount rotation capability but also have independent tip/tilt adjustment capabilities and common focus adjustment of the entire array mount. Most of the optical components were received as the project went into a hibernation period due to a temporary lack of funding, therefore documentation of some deliverables was found to be incomplete.

Using the design model made in Zemax, a simple tolerance exercise was used to understand the bounds of the incoming field using estimated alignment errors added to the focus parabola. Using an angular alignment tolerance of the focus parabola of ± 2 arcmin in each axis, the allowable field-of-view into the spectrograph is 1.8 arcmin. For a simple laser beam alignment this is difficult but not impossible to meet.

3.1 Alignment of the central beam path

Figure 4 shows the elements used for setting the alignment into the system. After this step the focusing/collimating OAP's and pinhole were installed. After the required rotation of the mount, the focused spot was off the pinhole vertically which was fixed by shimming the mount. The resulting shear plate interferograms (Figure 5) show defocus and astigmatism. The location bushing was removed from one OAP mount but small amounts of movement did not seem to affect the shear plate interferograms. Another attribute of the parabolas is clearly seen in the images. The interference patterns show mid-spatial frequency errors which can also be seen in the areas not being interfered.

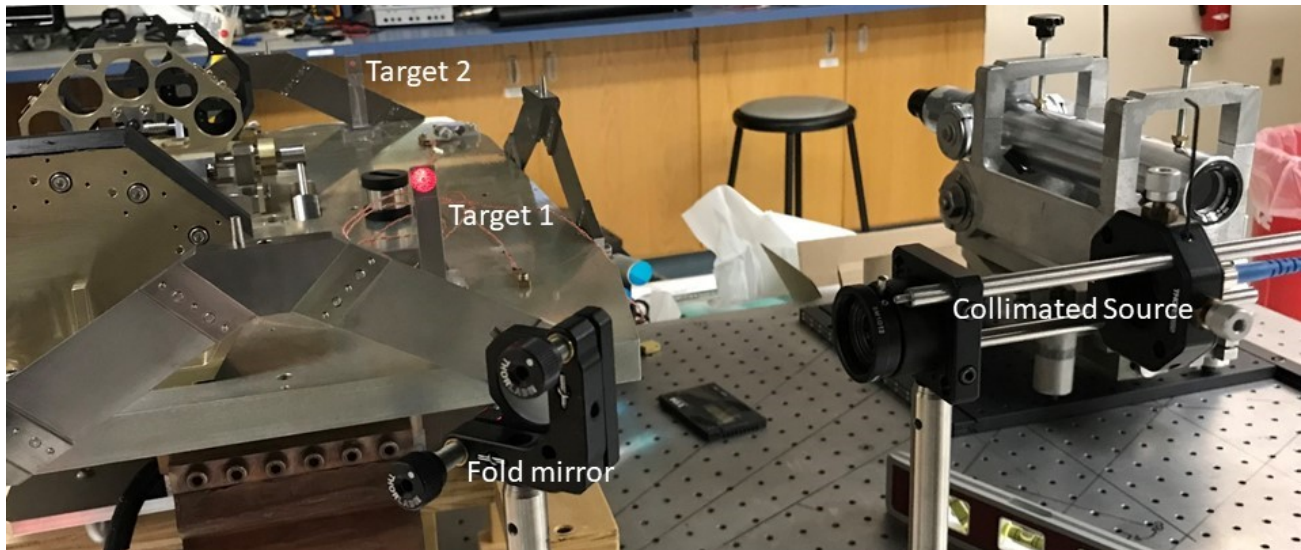


Figure 4. Initial alignment setup showing collimating system, fold mirror and first two targets. This first setup allows alignment of one incoming beam to the system.

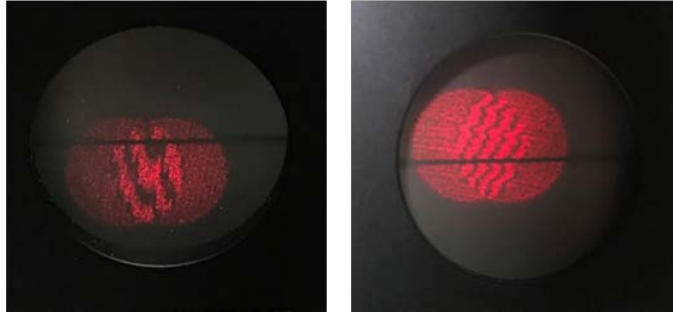


Figure 5. Orthogonal shear plate interferograms, after the collimating OAP, showing defocus and astigmatism. Also mid-spatial frequency errors from the machining process can be seen as fine lines which are adding the squiggles to the interference fringes.

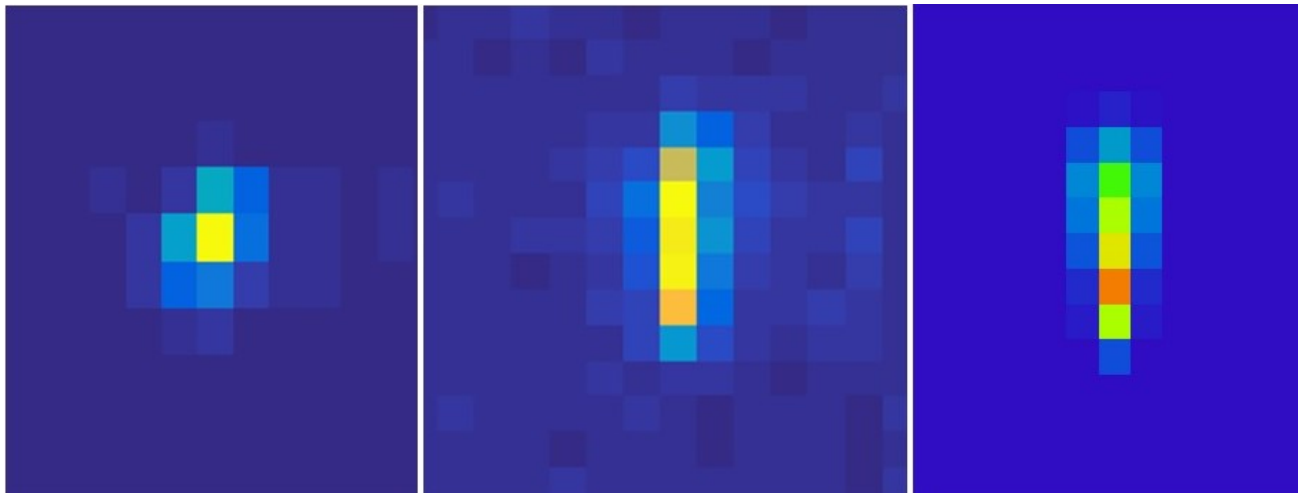


Figure 6. Left: white light image near best focus; middle: dispersed image from 1.50 – 1.68 microns; right: Zemax simulation of dispersed image.

Measurements were taken at the detector plane also using an uncooled Xenics Bobcat 320 to get a baseline image quality at the operable wavelengths. The test beam collimation was readjusted for 1.55 microns. A long wavelength pass filter was used with cut-on wavelength of 1.5 microns. The Xenics Bobcat 320 has a long cut-off wavelength of 1.68 microns; therefore, a working pass band from 1.50 – 1.68 microns. Figure 6 shows measured white light image, measured dispersed image, and Zemax simulation of dispersed image. The image could not be maximized in focus as the camera was not originally intended for this purpose and lacked the compactness to fit into the envelope; it ran into a stop before reaching best focus. An estimate of the ensquared energy of the image on the left is 40%, the design model shows a greater than 80% ensquared energy for the Bobcat pixel size. This is to be expected since there is astigmatism present and the stage ran out of motion. The middle picture in figure 6 shows the dispersed image taken with the camera. A model was built in Zemax to simulate the expected image. Running a few different dispersions showed the design and measured dispersion to be within 15%. In the future a measurement will be performed at cryogenic temperatures with narrowband filters to better quantify the true dispersion.

3.2 Alignment of the central three beam paths

The periscope system for steering the beams from the beam combiner to the spectrograph has not been purchased yet. For the initial alignment, we are using a large diameter collimated beam, shown in figure 7, which guarantees the input beams are parallel so that manufacturing errors causing mis-pointing can be seen. Initial measurements of beamlines 2 and 4 show astigmatism as in the central beam but at different angles. Checks on the manufacturing errors of the mounts and optics are being investigated.

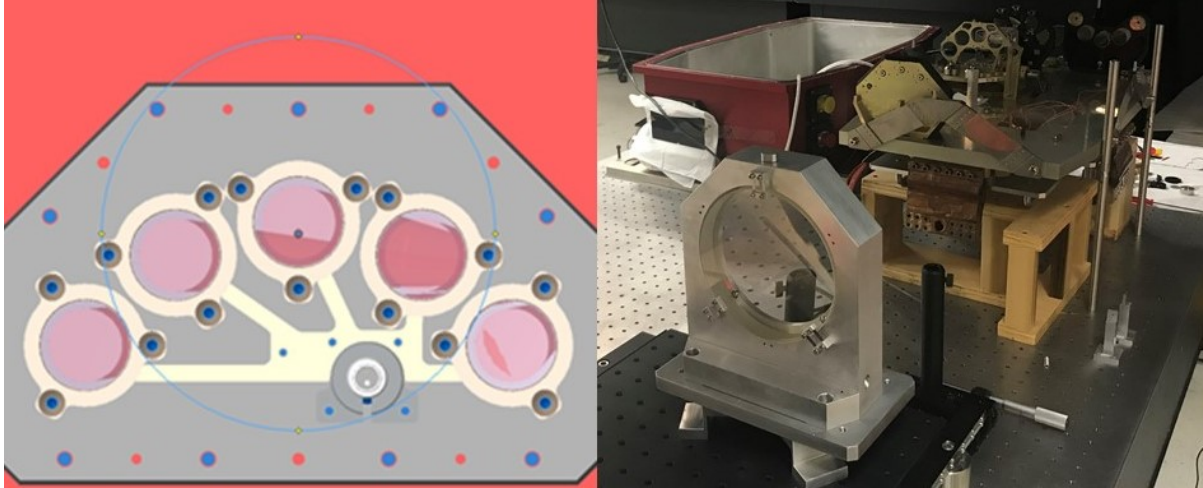


Figure 7. Stimulus for alignment and image verification for three beams. Left: Drawing showing clear aperture of lens and three initial beam paths. Right: Setup used to send three parallel beams into the system. Irises were also installed to limit the beam diameters to the actual diameters used in practice.

4. CONCLUSIONS AND FUTURE PLANS

After many years, the fringe tracking spectrograph is again under testing. At the same time mechanical redesign has happened to allow the incorporation of the much more appropriate SAPHIRA detector. The mount for the SAPHIRA detector is finished and a design to tilt the PICNIC test detector the same amount is being done. Modifications to the focus parabola mounts were tested on the first beamline and now are being machined for the next two beamlines.

Initial measurements of image quality are both good and bad. The interferograms show the presence of astigmatism that needs to be addressed but the preliminary image of the middle beamline at the detector looks promising. Testing and measurements of components will continue to narrow down the possible culprits so a solution can be formulated.

Future work will include cryogenic tests for image quality and throughput. Once the periscope optics and a multi-beamline stimulus arrive, the beam combining system will be restarted and systems tests be performed in anticipation of the SAPHIRA detector and electronics arriving in middle of 2019.

5. ACKNOWLEDGEMENTS

This material is based on research sponsored by Air Force Research Laboratory (AFRL) under agreement number FA9453-15-2-0086. The U.S. Government is authorized to reproduce and distribute reprints for Governmental purposes notwithstanding any copyright notation thereon.

The views and conclusions contained herein are those of the authors and should not be interpreted as necessarily representing the official policies or endorsements, either expressed or implied, of AFRL and or the U.S. Government.

REFERENCES

- [1] Jurgenson, C. A., Santoro, F. G., Baron, F., McCord, K., Block, E. K., Buscher, D. F., Haniff, C. A., Young, J. S., Coleman, T. A., and Creech-Eakman, M. J., "Fringe Tracking at the MROI," Proc. SPIE 7013, 70130C (2008).
- [2] Santoro, F. G., Olivares, A. M., Salcido, C. D., Jimenez, S. R., Sun, Xiaowei, Haniff C. A., Buscher, D. F., Creech-Eakman, M.J., Selina, R. J., McCracken, T., Young, J. S., Fisher, M., Klinglesmith, D., Torres, N. C., Dahl, C., Shtromberg, A. V., Wilson, D. M., "Final mechanical and opto-mechanical design of the Magdalena Ridge Observatory interferometer," Proc. SPIE 8445, 84452K (2012).

- [3] Jurgenson, C., Santoro, F., McCracken, T., McCord, K., Shtromberg, A., Klinglesmith, D., Olivares, A., Buscher, D., Creech-Eakman, M., Haniff, C., and Others, "The MROI fringe tracker: first fringe experiment," Proc. SPIE 7734, 773446 (2010).
- [4] McCracken, T., Jurgenson, C., Santoro, F., Shtromberg, A., Torres, N., Dahl, C., Farris, A., Buscher, D., Haniff, C., Young, J., Seneta, B., Creech-Eakman, M., "The MROI fringe tracker: Closing the loop on ICoNN," Proc. SPIE 8445, 84451N (2012).
- [5] Finger, G., Baker, I., Alvarez, D., Ives, D., Mehrgan, L., Meyer, M., Stegmeier, J., Weller, H., "SAPHIRA detector for infrared wavefront sensing," Proc. SPIE 9148, 914817 (2014).
- [6] Atkinson, D., Hall, D., Baranec, C., Baker, I., Jacobson, S., Riddle, R., "Observatory deployment and characterization of SAPHIRA HgCdTe APD arrays," Proc. 9154, 915419 (2014).